Reflection Interference Contrast Microscopy Combined with Scanning Force Microscopy Verifies the Nature of Protein-Ligand Interaction Force Measurements

J. K. Stuart and V. Hlady
Department of Bioengineering, University of Utah, Salt Lake City, Utah 84112 USA

ABSTRACT The integration of a stand-alone scanning force microscope (SFM) scanner with a reflection interference contrast microscope (RICM) makes it possible to measure directly the separation distance between the SFM probe and the sample surface. The SFM-RICM combination, when applied to the force measurements between ligand-derivatized SFM probe and a protein receptor-derivatized surface, showed that the anomalous force discontinuities often observed for such interacting pairs were indeed a real behavior characteristic of a particular experimental configuration. Apart from small discrepancies due to transient damping, commercially available cantilevers did behave in an ideal mechanical fashion, thus indicating that protein-ligand unbinding events were occurring at distances much larger than their maximum extended length. This external verification of separation distance requires a closer examination of the physical events occurring upon detachment of the surfaces. An alternative interpretation of such force measurements is proposed here in which the protein and/or ligand immobilization chemistry is called into question.

INTRODUCTION

Recently, the use of scanning force microscopy (SFM) to measure interaction forces between molecular recognition pairs has been reported by several research groups (Allen et al., 1997; Boland and Ratner, 1995; Chilkoti et al., 1995; Dammer et al., 1995; Florin et al., 1994; Hinterdorfer et al., 1996; Lee et al., 1994a,b; Stuart and Hlady, 1995). By immobilizing specific receptor moieties to a substrate surface and the corresponding ligand to the SFM probe, it is possible to generate a distinguishable tension between the pairs as they are separated, thus quantifying the forces and energies required to dissociate bound molecules. Using this tool, one can possibly map the distribution and functionality of a biomolecular surface on a very small scale, potentially detecting only a few receptors at a time. This concept is currently being utilized in the development of a hand-held multichannel force-amplified biosensor (Baselt et al., 1996).

Molecular affinity SFM technology has been applied using various physical configurations and chemical immobilization techniques. Substrate materials have ranged from silicon-based surfaces (Allen et al., 1997; Stuart and Hlady, 1995) to agarose beads (Florin et al., 1994). Molecules have been attached to the substrate surface covalently with polymeric linkers (Hinterdorfer et al., 1996; Stuart and Hlady, 1995) or by affinity techniques such as "sandwich" configurations, in which ligands are bound to the surface through covalent grafting (Florin et al., 1994), physisorbed liganded bovine serum albumin (Chilkoti et al., 1995; Lee et al., 1994b), self-assembled monolayers (Dammer et al., 1996), or antibodies (Hinterdorfer et al., 1996). Reactive moieties have also commonly been directly immobilized to a surface by physisorption. Numerous molecular pairs have been studied, including cell adhesion proteoglycans (Dammer et al., 1995) and DNA oligonucleotides (Boland and Ratner, 1995; Lee et al., 1994a), in addition to biotin-streptavidin (Chilkoti et al., 1995; Florin et al., 1994; Lee et al., 1994b; Moy et al., 1994) and antibody systems (Allen et al., 1997; Dammer et al., 1996; Stuart and Hlady, 1995). Most studies have used ligands immobilized directly to the silicon nitride SFM cantilever tip, although several, including that reported here, have immobilized ligands to a small spherical probe, which is subsequently attached to the apex of the cantilever.

While commercial SFM instruments are in many ways well suited to these investigations, there are several drawbacks to using the SFM for measuring molecular interactions. The chemical methods used to immobilize the binding pairs can sometimes generate spatial or functional uncertainty. Small-scale inhomogeneities in the substrate surface will translate into an inhomogeneous molecular layer, making quantification of single-molecule interactions possible only through a large number of measurements, i.e., through statistical averages. Random orientation of immobilized molecules can also create variability in binding efficiency and rupture force. Ideally, oriented monolayers will result in less uncertainty. Physisorption of receptors can also result in variability; in addition to slow desorption and decay of the reactive layer, proteins can also bind nonspecifically to a surface, denature, and be rendered nonfunctional. When this is the case, the unfolded protein may adhere to the tip nonspecifically, causing unpredictable background forces. Background interactions generated by the physical nature of

Received for publication 23 January 1998 and in final form 1 October 1998.

Address reprint requests to Dr. Vladimir Hlady, Department of Bioengineering, University of Utah, 108A Biomedical Polymers Research Building, Salt Lake City, UT 84112. Tel.: 801-581-5042; Fax: 801-585-5151; E-mail: vladimir.hlady@m.cc.utah.edu.

Dr. Stuart's present address is Structural Biology Program, The Burnham Institute, La Jolla, CA 92037.

0006-3495/99/01/500/09 $2.00

the linker molecules themselves can also be significant and sometimes unavoidable. For instance, experiments have been reported in which the surface forces apparatus was used to determine that disruption of a self-assembled molecular lipid layer was occurring between the lipid anchors and not at the recognition site (Leckband et al., 1995). It is therefore important to characterize background forces and to be able to distinguish them from specific forces.

Most of the literature on molecular affinity SFM has reported a rather long-range discontinuous adhesion behavior. Many groups attribute the reproducible "jumpy" nature of force versus separation ($F(s)$) measurements to the unbinding of receptor-ligand pairs, which for the most part is consistent with a theoretical model of measurement results. However, this interpretation is tested in the present work, as the unbinding events measured occur at distances that would stretch the immobilized molecules to tens of times their original dimensions, conditions that normally result in loss of functional specificity. In fact, Rief et al. have published $F(s)$ profiles highly similar to the ones seen using affinity pairs for a nonspecific system in which the unfolding of individual domains of titin protein resulted in discrete force jumps (Rief et al., 1997). It is clear that most specific receptor-ligand systems require retention of their three-dimensional conformation to function properly. Therefore, throughout this work, an alternative interpretation of adhesion force measurements will be explored, using the integration of reflection interference contrast microscopy (RICM) for an independent characterization of separation distance.

RICM has been elegantly applied to a similar system in which a latex microprobe is attached to a cell/vesicle transducer surface through biospecific adhesion (Evans et al., 1995). The vertical movement of this microprobe is monitored by observation of changes in interference fringe patterns, and forces applied to the probe are quantified via video imaging of changes in the cell transducer radius, which is proportional to its stiffness. Adhesion forces can be quantified using this technique over a range of 1 nN to 0.01 pN, whereas the SFM is only sensitive to ~0.01 nN, the strength of a weak noncovalent bond (Bell, 1978). The application of RICM to our molecular affinity SFM studies allows the measurement of probe-sample separation to a vertical (z) resolution of ~4–10 nm. By using the SFM cantilever as a transducer, one can securely attach a covalently liganded microprobe to it, thus eliminating the possibility of rupturing membrane-bound receptors. In addition, the detection scheme used by most SFM instruments is straightforward and capable of quantifying physical information in three-dimensional space.

Commercial SFM instruments generally use an optical lever detection scheme, which calculates force, using Hooke's law, as a function of the angle change of the cantilever upon deflection. This method is simple and effective for small-angle changes, but it does not provide the independent measure of probe-sample separation distance that is necessary to determine the behavior of the cantilever. The optical lever technique assumes that probe-sample separation is equivalent to the difference between the piezo travel and the cantilever deflection, although some instruments display force measurements as a function of piezo travel alone (this has a direct correlation to the time course of the experiment). The above assumption holds true if the cantilever behaves as an ideal beam; this is the hypothesis being tested in this work.

Reflection interference contrast microscopy

Recent developments in the commercial SFM scanner have made available a stand-alone, portable scanning head in which the cantilever chip itself is mounted to the piezoelectric transducer, affording x-y-z movements while leaving the underside free for integration with samples of almost any size or configuration (van der Werf et al., 1993). This setup is ideal for integrating the SFM with an inverted optical microscope for simultaneous visualization of biological structures (Putman et al., 1992). Any variation on optical spectroscopy is thus possible; one can compare properties using fluorescence, evanescent spectroscopy, phase contrast, or confocal scanning microscopy. The application of RICM has been reported as a combined method for determining bead height in an SFM area image (Hillner et al., 1995). We have recently published results using RICM to determine bending or instabilities along the length of a rectangular cantilever during a receptor-ligand adhesion measurement (Hlady et al., 1996). We report here an extension of these studies, resulting in the novel use of RICM for independently determining SFM probe-sample separation during $F(s)$ measurements.

The principle of RICM is shown in Fig. 1 and is described in detail by Tolansky (1973). The object, which in this case is a spherical glass bead glued to the SFM cantilever, is observed through the microscope objective, using epiillumination with relatively monochromatic light. The incident beam, I_0, is partially reflected at the coverslip-buffer interface, I_{12}, and partially transmitted through the buffer to be reflected by the bead. The constructive or destructive interference pattern formed by the superposition of the object beam, I_{23}, and the reference beam, I_{12}, is observed again in the objective as circular interference fringes, which are a function of distance between the bead and surface. The vertical distance, d, between each fringe is calculated as $d = a\lambda/2n$, where a is the fringe number, n is the refractive index of the buffer medium ($n = 1.33$ for water), and λ is the wavelength of the monochromatic light, for example $\lambda = 488$ nm in our case. Thus, in aqueous solution the vertical distance between each dark fringe corresponds to 183.5 nm.

The intensity at each point in the pattern is of the form (Rädler and Sackmann, 1992)

$$I(z) = I_{12} + I_{23} + 2\sqrt{I_{12}I_{23}}\cos[(4\pi n_2/\lambda)(g(z) + h) + \delta] \quad (1)$$

where n_2 is the refractive index of the buffer medium, δ is the phase shift that occurs at the buffer-bead interface

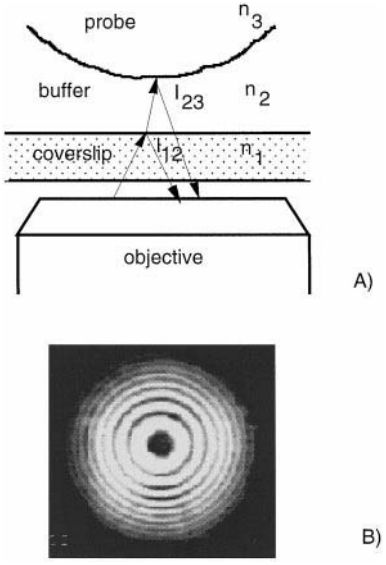

FIGURE 1 Principle of reflection interference contrast microscopy. (*A*) The incident beam is partially reflected at the coverslip-buffer interface, I_{12}, and partially transmitted through the buffer to be reflected by the probe, I_{23}. The constructive or destructive interference pattern formed by the superposition of the object beam, I_{23}, and the reference beam, I_{12}, is observed through the objective as in *B* as circular interference fringes, which are a function of vertical distance between the spherical probe and surface.

(which is equal to π here, because the bead has a higher refractive index), h is the minimum separation distance between the sphere and surface, and $g(z)$ describes the contour of the bead as

$$g(z) = R - \sqrt{R^2 - z^2} \quad (2)$$

where R is the radius of the bead. By measuring the intensity at any point in an RICM image, therefore, the bead-sample separation can be calibrated. This information can be applied in conjunction with the SFM force measurement data to decipher the relationship between the unbinding force and the separation distance between the two interacting objects.

The variance in interference patterns measured with RICM can be due to several factors. Stray light can create a large background signal but can be minimized with a series of polarizers (Rädler and Sackmann, 1992). The absolute distance determination can be affected by the numerical aperture of the illumination or the focus of the objective. Because of the incoherent illumination, there is a rapidly decaying visibility of higher order fringes; this is termed the finite illumination aperture effect (Rädler and Sackmann, 1993). The presence of a surface film will affect the optical path length if it has an index of refraction different from that of the buffer. This can be accounted for in the computation of minimum separation.

The RICM technique has been used effectively to measure vesicle spreading (Sackmann, 1996) and colloidal forces (Rädler and Sackmann, 1993), among others. Its use in determining cantilever deflection and bending is also described by Hlady et al. (1996). It is estimated that RICM has a spatial resolution (i.e., in x,y) of ~300 nm and a vertical (z) resolution of ~4 nm (Sackmann, 1996), making it all the more ideal for combination with SFM force-separation measurements.

To answer questions regarding probe-sample separation and cantilever behavior, we integrated the SFM with the RICM. This combination was used to study interaction forces and distances between receptor/ligand pairs. The example system presented here uses antifluorescyl IgG/fluorescein pairs covalently immobilized to glass or quartz substrates with a glycidoxypropylsilane (GPS) linker (Stuart, 1997). The fluorescein ligand was immobilized to a glass sphere, which was subsequently glued to the apex of a commercial SFM cantilever. By using RICM as an external characterization technique, the nature of the immobilized surface films can be appropriately analyzed.

EXPERIMENTAL

Sample derivatization and characterization

Glass coverslips (1″ round) and glass beads (5–50 μm) were prepared as detailed by Stuart (1997) and Stuart and Hlady (1998). Briefly, the substrates were covalently derivatized with 3-glycidoxypropyltrimethoxysilane (GPS) (Hüls/United Chemical Technologies, Bristol, PA) to create an amine-reactive surface film. Proteins or ligands were immobilized directly to this layer through a carboxydiimidazole (CDI) (Pierce Chemical Co., Rockford, IL) cross-linker. The monoclonal antifluorescyl IgG (kindly provided by Dr. J. Herron, University of Utah) was randomly bound through primary amines at a pH of ~8.5. The ligand used was 5-(((2-(carbohydrazino)-methyl)thio)acetyl)aminofluorescein (Molecular Probes, Eugene, OR).

Both substrate and probe were thoroughly characterized to establish the effectiveness of the surface chemistry (Stuart, 1997). Contact angle measurements monitored changes in the surface energy of each layer, and x-ray photoelectron spectroscopy quantified the elemental compositions. Total internal reflection fluorescence and fluorometric measurements were performed as an external means of verifying functionality and kinetics of the IgG binding.

The roughness of clean glass substrates was measured using the SFM standard cantilever with integral tip; upon acquisition of an area image, surface topography and rms roughness could be quantified with Explorer software. The roughness of the spherical glass probes was assumed to be similar to that of the coverslips. The shape and correct placement of the probe on the cantilever was observed in a scanning electron micrograph (not shown).

Probe attachment

Before each experiment, 20-μm glass spheres derivatized with the appropriate ligand were glued to the apex of clean, commercially obtained SFM cantilevers (Park Scientific, Santa Clara, CA). A 1-μm-diameter tungsten wire was secured to the arm of a three-stage micromanipulator (461 Series; Newport, Irvine, CA) and was used to apply a small droplet of a two-part adhesive (Locquic Activator 707 and Speedbonder 325; Loctite Corp., Newington, CT). New wires were then used to transfer single spheres electrostat-

ically onto cantilevers with appropriate spring constants (0.02–0.1 N/m).

Integration of SFM and RICM

The stand-alone Topometrix Explorer SFM scanner allows for convenient integration with an inverted microscope by simply placing it on the microscope stage, where the cantilever can be imaged from its underside. Because of this capability, interference measurements can easily be made simultaneously with SFM measurements. The schematic of the SFM/RICM setup is shown in Fig. 2.

A custom-made open fluid cell was machined from Teflon for this purpose. It was designed to hold a standard 1″ round glass coverslip, which was pressed into a custom-made plate and fit onto the stage of a Nikon Diaphot 200 inverted microscope. In all cases, phosphate buffer solution (10 mM phosphate buffer, pH 7.4, 25 mM NaCl) was added to the cell before the cantilever probe was submerged in position. For some positive controls, bulk ligand was also added to the buffer solution. A 488-nm bandpass filter was inserted into the reflected light path of an Hg lamp to create a somewhat monochromatic source. Both field and aperture irises were kept closed to quasicollimate the light. A 100×, 1.25 N.A. oil immersion objective (Leitz) was used to image the probe movement optically. A CCD camera (Hamamatsu C2470; Hamamatsu Photonics, Bridgewater, NJ) was fitted into the side camera port and connected to an image processor (Argus 20; Hamamatsu Photonics), making it possible to visualize the experiments on a video monitor and record them on videotape with a video cassette recorder.

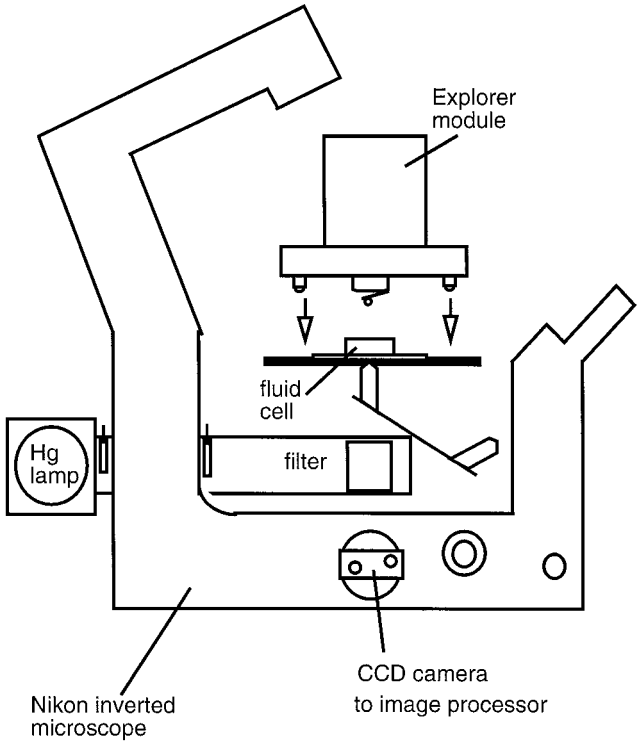

FIGURE 2 Schematic showing integration of SFM with RICM. The Explorer stand-alone SFM scanner is placed on the stage of an inverted microscope such that the spherical probe is in proximity to the imaged surface. Optical fringes are recorded in real time through a CCD camera inserted in the microscope side port.

Data collection

SFM force-displacement measurements were recorded simultaneously with RICM video footage. Time was used as a common parameter so that the two measurements could be correlated by activating the image processor's timer on the video screen. Experiments were performed at a piezo travel rate of 300 nm/s. Multiple single $F(s)$ measurements were obtained, in which upon activation the probe would travel from its resting position, some distance from the surface, to the point of contact, after which the displacement of the piezo over the specified travel distance was allowed to increase the load of the probe to the sample surface. The probe was then retracted away from the surface, changing the positive load at the point of the contact into negative load (i.e., tension). The magnitude of the tension required to detach the probe from the surface (i.e., the adhesion force) was recorded using the SFM optical lever method while the probe's interference fringes were simultaneously videotaped. This process was repeated a number of times, after which the probe was either moved to another location or removed entirely to change the fluid medium. The attempt was made to minimize damage to the proteins and surface film that could be caused by repeated pressure and forced unbinding by the probe. It has been shown that as few as 10 repetitions are sufficient to collect meaningful information on force versus variance (Williams et al., 1996); therefore, 3–10 measurements (consisting of multiple force jumps) were made at each location.

Data analysis

To determine separation distances accurately in $F(s)$ measurements, probe-sample separation was recalculated as the difference between the movement of the piezoelectric transducer (calculated from the applied voltage to the piezo) and the deflection of the cantilever (measured by the SFM optical lever technique). This determination differs from force versus piezo displacement measurements ($F(d_p)$) frequently reported in the literature in which the abscissa is shown as only piezo displacement and is proportional to time. A typical $F(s)$ measurement is shown in Fig. 3, in which unbinding forces can be correlated with theoretical probe-sample separation distance. To compare unbinding events to the separation distance obtained from RICM experiments, the $F(d_p)$ measurements were used, as the interference fringe data are also proportional to time.

Interference fringe information was extracted and digitized from the videotapes using a Macintosh PowerMac computer with a frame grabber card (L-3; Scion Corp.,

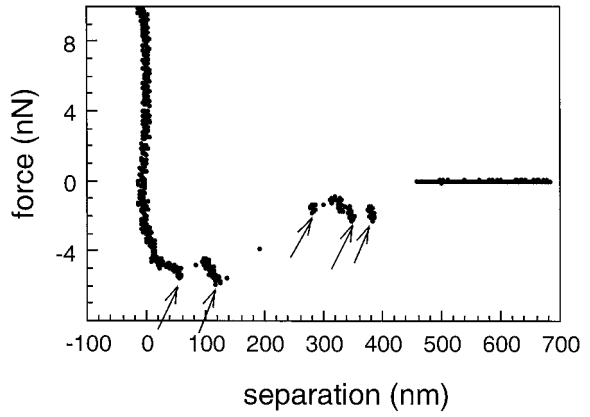

FIGURE 3 A representative $F(s)$ measurement between a GPS-antifluores-cyl IgG surface and a GPS-fluorescein probe. The force discontinuities due to unbinding events are identified by arrows.

Frederick, MD) and National Institutes of Health/Scion Image 1.57 software. The videos were played on the computer screen to locate the segment of interest. A selection tool was used to choose a section in the center of the bead that was two pixels in height and included the bead apex, as shown in Fig. 4 *A*. The Image software was used to extract information from only this section for a chosen number of frames, which were taken with a time resolution of 70 ms. A montage of this sequential series of two-pixel cross-sectional frames was then constructed, which enabled a visualization of the fringe progression with time across the center of the bead (see Fig. 4 *B*). The Hg lamp could be seen to fluctuate in intensity over the course of the experiment. To minimize this interference, montages were normalized by subtracting a background section from the entire image, termed "flat-fielding."

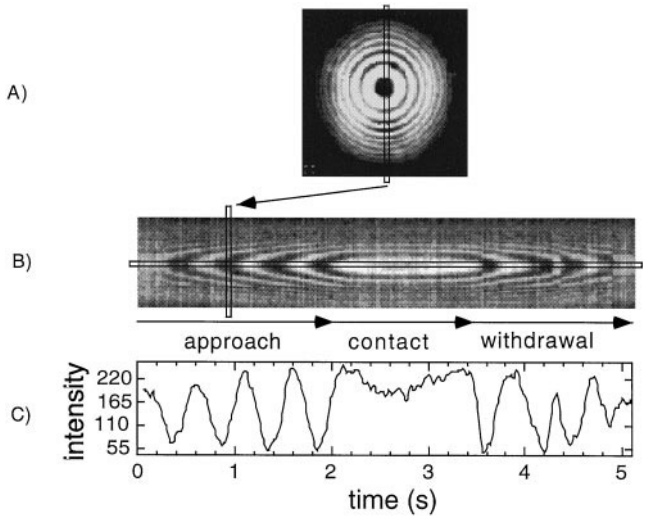

FIGURE 4 Interpretation of RICM measurements. (*A*) Instantaneous interference fringe pattern of the SFM spherical probe. A two-pixel cross section of its diameter is taken every 0.07 s as the probe approaches, contacts, and withdraws from the sample, shown stacked sequentially in the montage (*B*). A profile of the intensity at the center of the probe shown in (*C*) is used to calculate the probe-sample separation distance at any point during the approach-withdrawal cycle.

As already described (under Reflection Interference Contrast Microscopy), the periodicity of an interference fringe scales with $\lambda/2n$. In this case, it is difficult to obtain high-resolution information on small z-movements using only the eye. Instead, a profile of the fringe intensity (i.e., in an 8-bit resolution of the image gray scale) over the measurement shown in the montage was obtained using the Image software (see Fig. 4 *C*). We have assumed that the apex of the bead movement through the vertical fringe space undergoes intensity changes that can be mapped by a normalized cosine function. Because of the decaying contrast with distance, the amplitude of the intensity will decrease with a certain envelope such that, according to Rädler and Sackmann (1992), the intensity should follow

$$I(x) = A_0 + A_1 e^{-b_1 z^2} + A_2 e^{-b_2 z^2} \cos[(4\pi n_2/\lambda)(g(z) + h) + \delta] \quad (3)$$

where A_0, A_1, and A_2 describe the amplitudes corresponding to the baseline, background, and decaying contrast due to diffuse reflection at higher separations, respectively, and b_1 and b_2 are exponential fitting parameters. We first used the approach part of the cycle to map the distances in the retraction part of the cycle as an intensity profile calibration for corresponding fringe order. This was necessary because, upon retraction, jumps out of contact could occur over distances covering the majority of or exceeding an entire cycle. For this reason, intensity profiles could not be easily fit to the above equation. Instead, a simple cosine function was applied to each half-cycle individually as

$$\theta = 2 \cos^{-1}[(I_{max} - I)/(I_{max} - I_{min})] \quad (4)$$

$$d = [(\theta/180)(\lambda/2n) + a\lambda/2n] \quad (5)$$

where a is the number of the cycles from contact, I_{max} and I_{min} are the maximum and minimum intensities recorded over the interval in question, respectively, and I is the intensity at the time point of interest. It is assumed that the error due to change in amplitude is negligible and noncumulative. These calculations can be accurate to ~10 vertical nm, depending upon how many points are in the half-cycle.

In evaluating the distances from RICM recordings, we have made the following assumptions: 1) in approaching the sample surface the cantilever chip travels through space with a uniform known velocity, i.e., there are no velocity variations due to hysteresis or creep of the piezo translator; 2) the apex of the sphere that will make contact is positioned in a fixed x and y location of the image as it is translated in z, i.e., there is no horizontal displacement; 3) the refractive index of the medium is constant; 4) the refractive index of adsorbed layers is the same as that of the medium; 5) overall variations in light intensity from the lamp are taken into account by the "flat-fielding" normalization procedure.

The aforementioned separation distances calculated from fringe intensity profiles can be compared with the separation calculated from $F(s)$ measurements, which involve a

jump out of adhesive contact accompanied by sometimes erratic behavior. From this information, it is possible to determine the absolute separation of the SFM probe at any time and whether this separation is accurately determined by the force measurement information.

RESULTS

The $F(s)$ measurement shown in Fig. 3 depicts the withdrawal portion only of a full adhesion measurement between a GPS-antifluorescyl IgG surface and a GPS-fluorescein probe, recalibrated to reflect probe-sample separation as determined by the SFM. These experiments were performed at a piezo travel velocity of 300 nm/s. The contact time varied slightly with each experiment, because of differences in the initial separation distance. In the experiment shown, the probe and sample were in contact for ~2 s. Other experiments were performed at velocities of 500 nm/s and 100 nm/s (not shown), and it was determined that there was no notable rate dependence to the measurements. This is probably because any specific bonds will be formed in a small window of time when the probe and sample are at an optimal distance from each other and will dissociate under stress at a rate much faster than that measurable here (Bell, 1978). However, an experiment in which the probe and sample were allowed to remain in contact for longer periods of time (i.e., 1–2 min; not shown) showed that adhesion magnitude and separation distance were both affected. This emphasized molecular rearrangements that are thought to occur that increase nonspecific forces, as the half-life of the IgG-fluorescein bond is on the order of 49 s (Kranz et al., 1981) and is calculated to be orders of magnitude lower than this under stress (Bell, 1978), i.e., specific bonds will break within a time period below that measurable with molecular affinity SFM. Therefore contact times were kept to a minimum as much as possible.

It can be seen in Fig. 3 that the final jump out of contact does not occur until ~450 nm separation according to the recalibration of intrinsic SFM data. The same data are shown again as a function of time (uncalibrated, proportional to piezo travel) in Fig. 5 *A*. Superimposed on this force measurement is the separation between probe and sample, calculated from the RICM fringe intensity data recorded during the same time interval. The fringe peaks (Fig. 5 *B*) are assumed to correspond to multiples of 183.5 nm and follow a sinusoidal pattern. This fringe intensity profile, shown in Fig. 5 *B* for the entire approach-withdrawal measurement cycle, is obtained by measuring the intensity variation along a cross section of the probe montage, shown in Fig. 5 *C*. The intensity profiles typically can be seen to show fluctuations in contact. This is partially due to the fact that the optical sampling results in averaging of sample distance for each point. Distances along the circumference of the bead could be noticeably different, largely because of the known roughness of the glass surfaces (~60 nm rms; Stuart, 1997) originating from surface asperities on a small scale, but also because of the heterogeneity in the thickness of the surface film.

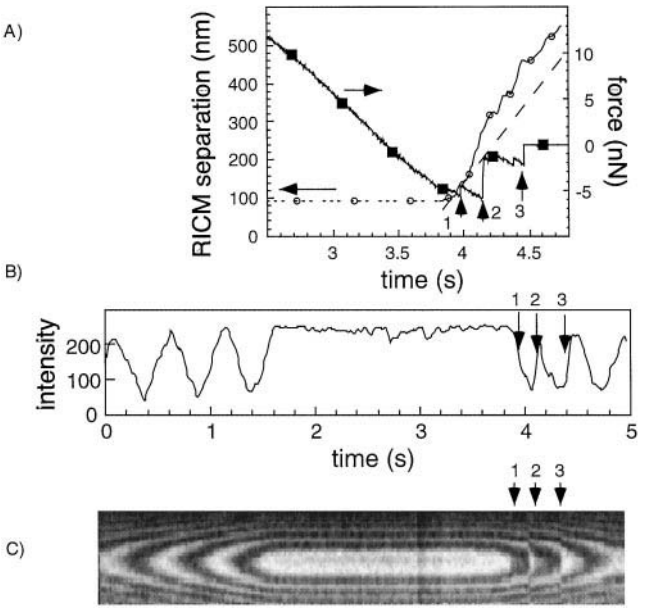

FIGURE 5 Results of an RICM measurement used to determine the separation distance between probe and sample with time. (*A*) Overlaid plots of a SFM $F(time)$ measurement (withdrawal portion, ■) and the corresponding separation, s (○), calculated from RICM data, using the intensity profile (*B*). The intensity profile was obtained from the center of the montage shown in *C*, generated as described in the Data Analysis section and Fig. 4 B. Arrows in the montage (*C*) indicate clear discontinuities, which are seen to correspond to discontinuities on both the force plot in *A* and the intensity profile in *B*. The dashed line in *A* represents the increase in separation distance with time that would occur if there were no force discontinuities.

Comparing the RICM-measured separation versus time to the SFM adhesion force versus time measurement (Fig. 5 *A*), it can be seen that the probe and sample remain in contact until the first small jump-out, which is shown as an increased upward slope (i.e., increased velocity relative to the theoretical separation distance increase occurring at constant velocity, indicated by the *dashed line*). After that the experimental velocity decreases momentarily at the same time as the force plot shows another downward deflection. The interpretation of force plots can be somewhat deceiving in this regard, in that a downward deflection may tend to be perceived as a negative change in separation, when it is more likely that the sample is continuing to travel further away from the probe, but an increase in tension is causing the cantilever to be pulled away from the sample with a transient slower velocity. At the next apparent large jump out of contact, the separation plot in Fig. 5 *A* shows an increase in velocity over a large distance of nearly 100 nm. This same separation is indicated in Fig. 3 as occurring over a distance of ~150 nm; thus, there are some small discrepancies in separation determinations during the course of the adhesion measurement. Several velocity decreases can be seen to occur at the same or similar times as the remaining discontinuities, between which the probe and sample con-

tinue to separate. At the final jump out of contact, there is a brief halt in separation (corresponding to a horizontal line). This is indicated to occur at the separation distance of ~450 nm, which is the same distance found in the $F(s)$ plot in Fig. 3. When the cantilever is at rest, the piezo is continuing to travel; thus the fringes indicate further separation.

Several discontinuities are also apparent on the montage, which are marked in Fig. 5 *C*. These discontinuities are fairly dramatic, and the first one to occur causes a jump of one full fringe cycle (i.e., 183.5 nm) in ~250 ms, as opposed to the corresponding approach cycle lasting ~500 ms/cycle. The location of these steps is indicated on the corresponding fringe profile. The transitions are subtle on the profile itself and correspond to increases in velocity, but the locations of these jumps can be more clearly seen to correspond to jumps on the $F(t)$ plot (Fig. 5 *A*).

DISCUSSION

The results from simultaneous SFM/RICM experiments indicate that all discontinuities apparently correspond to increases in separation between the probe and sample. We have previously proposed an alternative explanation for anomalous force-separation behavior in which lateral forces between the probe and sample could cause the cantilever to bend in such a way that there is a false indication of separation distance (Stuart and Hlady, 1995). One could argue that distances calculated using RICM may also be erroneous because of the possibility of force discontinuities occurring faster than the rate of data acquisition (i.e., faster than 70 ms). If the cantilever jumps over distances greater than half a fringe cycle (i.e., 92 nm) in this time, one cannot distinguish whether the jump was toward or away from the surface. However, even dramatic jumps such as those in Fig. 5 *C* appear to occur over time periods several times longer than the acquisition rate limitation. Moreover, a lateral movement of the probe would result in a change in cantilever deflection while the surfaces remained relatively close in contact. One would not expect vertical changes on the order of 100 nm to occur because of "rolling" of the probe; moreover, no lateral movement is detected in the video montages (Figs. 4 *B* and 5 *C*). Furthermore, the likelihood of agreement between the two methods, one of which is determined radially and one normally, would be low if the cantilever were behaving nonideally.

Small discrepancies are observed between the separation distances determined with the two methods during the transition from contact to complete separation (Figs. 3 and 5 *A*). This emphasizes that although the cantilever behavior is not erratic, there is some time-dependent behavior or damping of the system. During this transition period, the exact cantilever conditions are difficult to determine by the traditional optical lever method, causing some potential error in correlation of force discontinuities with separation distance. Integration with RICM is therefore a powerful technique for determining the behavior of surface films during force measurements between biological molecules.

The total separation distances upon the final jump out of contact measured by recalculated SFM and RICM correspond exactly. Therefore any nonideal cantilever behavior is compensated for by this time. It can be concluded that even though the SFM optical lever technique measures overall separations and forces accurately, the physical behavior during the transition out of contact, which is usually the period of most interest, is not determined accurately. The large separation distances measured for these samples are real, and these measurements show that the biopolymer film is being stretched over such a distance.

With this information, the results of molecular affinity SFM measurements should be evaluated carefully. The large separation distances measured indicate that molecular layers are being stretched seemingly beyond their limits. The GPS molecule itself has dimensions of only a few Ångstroms, and the proteins are ~6–10 nm in size over the longest dimension in their native conformation. If one were to unfold one of these molecules completely to a linear chain, it still would not cover the 400–500-nm distances measured with the SFM/RICM. If, theoretically, the protein were stretched to a linear chain, it is highly doubtful that it would retain its recognition capabilities.

The most logical conclusion to be drawn is that the GPS-protein layer is being delaminated from its surface. If the trifunctional siloxane groups of GPS were to cross-link horizontally because of condensation reactions, as is generally the case, then a film of GPS, continuous over some distance, would be formed. During intermediate derivatization steps, which are often performed in aqueous solution, the siloxane bonds formed with the glass surface could be hydrolyzed, thus allowing the film to delaminate in patches of at least 500 nm. This is especially the case for glass surfaces in which heterogeneously distributed patches of other less reactive metal oxides can be present in addition to silicon dioxide.

Assuming this to be the case, the covalent silane chemistry would seem to be detrimental to performing reliable molecular affinity SFM measurements. The presentation of proteins for proper specific interaction with ligand may also be compromised by the roughness of both surfaces; a 10-nm protein could potentially be inaccessible to the probe if it is located inside a 60-nm well. Thus the effective number of receptor-ligand interactions may be fewer than that indicated by characterization experiments where one component is in solution. However, for surfaces derivatized with polymer or protein, the contact area will be increased and will become more uniform because of the viscoelastic nature of the film. This "soft" surface only partially compensates for the heterogeneous nature of the samples, both topographically and chemically. Therefore the interactions were analyzed in a statistical way; as mentioned, 3–10 experiments were performed at each location, and multiple locations were sampled for each data set. The measurements performed did show some statistical differences in specific experiments compared to controls (data not shown) (Stuart, 1997; Stuart and Hlady, 1998). Specific fluorescein-IgG

measurements resulted in an overall mean force magnitude of 2.19 nN, versus negative control force measurments between a GPS-fluorescein probe and a GPS surface bearing nonspecific protein (adsorbed avidin), which resulted in a mean force magnitude of 1.01 nN, and positive controls in which bulk fluorescein added to the buffer solution resulted in reduced average force magnitudes of 0.95 nN. It is possible that affinity bonds can be formed on top of the film layers, which increases the potential delamination force, although it is not unlikely that the proteins are stretched or denatured in addition to the surface film. With a heterogeneous surface, nonspecific adsorption and denaturation of proteins, and/or bridging of molecules from one surface to the opposing one, is more probable.

CONCLUSIONS

The integration of RICM with SFM can be a highly useful tool in determining the physical nature of recognition events. Its use has shown that commercial SFM cantilevers do behave as relatively ideal beams and that lateral or frictional forces do not play a significant role in adhesion measurements. It has also shown that probe-sample separation distances are not determined with accurate resolution, as depicted by standard force versus piezo displacement plots. Their conversion into the $F(s)$ plots to include the effects of cantilever deflection does improve this determination, although damping or hysteresis in the cantilever can cause discrepancies of tens of nanometers during the course of separation. The most significant conclusion to be drawn from RICM/SFM data is that overall separation distances are indeed real, albeit in a range that is biologically unrealistic.

Long-ranged, discontinuous adhesion force profiles are routinely observed during SFM measurements of specific protein-ligand interactions. Although these discontinuities can be interpreted as specific unbinding events, and certainly thorough statistical analyses have determined that adhesion measurements show discrete or quantized behavior, it is suggested that a more rigorous analysis be applied to the physical interpretation of these data. Methods and control experiments to distinguish nonspecific background contributions (such as biopolymer unfolding or delamination) from specific unbinding events must be applied when separations occur over distances that are unlikely to correspond to functional molecular events in vivo. The accurate determination of forces and energies corresponding to single dissociation events is an exciting prospect, as techniques are continually being developed to improve the understanding of these measurements.

The authors acknowledge discussions with Dr. Clayton Williams and financial assistance from the Center for Biopolymers at Interfaces, University of Utah. This study was supported by National Institutes of Health grant HL44538.

REFERENCES

Allen, S., X. Chen, J. Davies, M. C. Davies, A. C. Dawkes, J. C. Edwards, C. J. Roberts, J. Sefton, S. J. B. Tendler, and P. M. Williams. 1997. Detection of antigen-antibody binding events with the atomic force microscope. *Biochemistry.* 36:7457–7463.

Baselt, D. R., G. U. Lee, and R. J. Colton. 1996. Biosensor based on force microscope technology. *J. Vac. Sci. Technol. B.* 14:789–793.

Bell, G. I. 1978. Models for the specific adhesion of cells to cells. *Science.* 200:618–627.

Boland, T., and B. D. Ratner. 1995. Direct measurement of hydrogen bonding in DNA nucleotide bases by atomic force microscopy. *Proc. Natl. Acad. Sci. USA.* 92:5297–5301.

Chilkoti, A., T. Boland, B. D. Ratner, and P. S. Stayton. 1995. The relationship between ligand-binding thermodynamics and protein-ligand interaction forces measured by atomic force microscopy. *Biophys. J.* 69:2125–2130.

Dammer, U., M. Hegner, D. Anselmetti, P. Wagner, M. Dreier, W. Huber, and H.-J. Guntherodt. 1996. Specific antigen/antibody interactions measured by force microscopy. *Biophys. J.* 70:2437–2441.

Dammer, U., O. Popescu, P. Wagner, D. Anselmetti, H.-J. Guntherodt, and G. N. Misevic. 1995. Binding strength between cell adhesion proteoglycans measured by atomic force microscopy. *Science.* 267:1173–1175.

Evans, E., K. Ritchie, and R. Merkel. 1995. Sensitive force technique to probe molecular adhesion and structural linkages at biological interfaces. *Biophys. J.* 68:2580–2587.

Florin, E.-L., V. T. Moy, and H. E. Gaub. 1994. Adhesion forces between individual ligand-receptor pairs. *Science.* 264:415–417.

Hillner, P. E., M. Radmacher, and P. K. Hansma. 1995. Combined atomic force and scanning reflection interference contrast microscopy. *Scanning.* 17:144–147.

Hinterdorfer, P., W. Baumgartner, H. J. Gruber, K. Schilcher, and H. Schindler. 1996. Detection and localization of individual antibody-antigen recognition events by atomic force microscopy. *Proc. Natl. Acad. Sci. USA.* 93:3477–3481.

Hlady, V., M. Pierce, and A. Pungor. 1996. A novel method of measuring cantilever deflection during an AFM force measurement. *Langmuir.* 12:5244- 5246.

Kranz, D. M., J. N. Herron, D. E. Giannis, and E. W. Voss, Jr. 1981. Kinetics and mechanism of deuterium oxide-influenced fluorescent enhancement of fluorescyl ligand bound to specific heterogeneous and homogeneous antibodies. *J. Biol. Chem.* 256:4433–4438.

Leckband, D. E., T. Kuhl, H. K. Wang, J. Herron, W. Muller, and H. Ringsdorf. 1995. 4–4-20 antifluorescyl IgG Fab′ recognition of membrane bound hapten: direct evidence for the role of protein and interfacial structure. *Biochemistry.* 34:11467–11478.

Lee, G. U., L. A. Chrisey, and R. J. Colton. 1994a. Direct measurement of the interaction forces between complementary strands of DNA. *Science.* 266:771- 773.

Lee, G. U., D. A. Kidwell, and R. J. Colton. 1994b. Sensing discrete streptavidin-biotin interactions with atomic force microscopy. *Langmuir.* 10:354–357.

Moy, V. T., E.-L. Florin, and H. E. Gaub. 1994. Intermolecular forces and energies between ligands and receptors. *Science.* 266:257–259.

Putman, C. A. J., K. O. van der Werf, B. G. de Grooth, N. F. van Hulst, F. B. Segerink, and J. Greve. 1992. Atomic force microscope with integrated optical microscope for biological applications. *Rev. Sci. Instrum.* 63:1914–1917.

Rädler, J., and E. Sackmann. 1992. On the measurement of weak repulsive and frictional colloidal forces by reflection interference contrast microscopy. *Langmuir.* 8:848–853.

Rädler, J., and E. Sackmann. 1993. Imaging optical thicknesses and separation distances of phospholipid vesicles at solid surfaces. *J. Phys. II.* 3:727–748.

Rief, M., M. Gautel, F. Oesterhelt, J. M. Fernandez, and H. E. Gaub. 1997. Reversible unfolding of individual titin immunoglobulin domains by AFM. *Science.* 276:1109–1112.

Sackmann, E. 1996. Supported membranes: scientific and practical applications. *Science.* 271:43–48.

Stuart, J. K. 1997. Feasibility of measuring protein interaction forces using a modified scanning force microscope. Ph.D. dissertation. University of Utah, Salt Lake City, UT.

Stuart, J. K., and V. Hlady. 1995. Effects of discrete protein-surface interactions in scanning force microscopy adhesion force measurements. *Langmuir.* 11:1368–1374.

Stuart, J. K., and V. Hlady. 1998. Feasibility of measuring antigen-antibody interaction forces using a scanning force microscope. *Colloids Surf. B.* (in press).

Tolansky, S. 1973. An Introduction to Interferometry. Longman, London.

van der Werf, K. O., C. A. J. Putman, B. G. de Grooth, F. B. Segerink, E. H. Schipper, N. F. v. Hulst, and J. Greve. 1993. Compact stand-alone atomic force microscope. *Rev. Sci. Instrum.* 64:2892–2897.

Williams, J. M., T. Han, and T. P. Beebe, Jr. 1996. Determination of single-bond forces from contact force variances in atomic force microscopy. *Langmuir.* 12:1291–1295.